Time-Efficient Quantum-to-Classical Data Decoding

Naveed Mahmud, Mingyoung Joshua Jeng, Md. Alvir Islam Nobel, Manu Chaudhary, SM Ishraq-Ul Islam, David Levy, and Esam El-Araby

University of Kansas, Lawrence, KS 66049, USA, {naveed_923, mingyoungjeng, islam.alvir, manu.chaudhary, ishraq, david.levy, and esam}@ku.edu

Abstract. A critical challenge for Noisy Intermediate-Scale Quantum (NISQ) devices is achieving time-efficient quantum state measurement or readout. Generally in quantum applications, data is encoded as the amplitudes of a superimposed quantum state. To extract information from the quantum state, the quantum circuit is sampled repeatedly, which incurs significant overhead in the system execution time. In this paper, time-efficient methods for decoding information from quantum states are proposed and evaluated. The process of extracting classical data from the quantum domain is termed in this work as quantum-to-classical (Q2C) data decoding. We propose a novel Q2C approach based on time-efficient sampling of quantum states using multi-level decomposable Quantum Wavelet Transform (QWT). Experimental evaluations of the proposed Q2C method are performed on a state-of-the-art quantum computing platform from IBM Quantum. Measurements of circuit execution time and circuit depth are obtained. Experimental results are consistent with our theoretical expectations and we present a quantitative comparison with existing techniques that confirm the efficiency of our proposed ap-

Keywords: Quantum Computing, Quantum Algorithms, Quantum State Preparation and Measurement

1 Introduction

Compared to classical computers, quantum computers are able to leverage unique quantum mechanical properties, i.e., superposition and entanglement, to achieve higher computational speedups [1]. Nevertheless, contemporary Noisy-Intermediate-Scale-Quantum (NISQ) devices have limited practical applications [2] due to significant challenges [3], one of which is efficiently decoding meaningful classical data from output quantum states. For example, in applications like quantum image processing, where information is usually encoded as the quantum state amplitudes [4], repeated sampling of the quantum circuit is required to generate a probability distribution from which the processed data can be recovered [5]. Such measurements often introduce a significant execution time overhead, necessitating the innovation of time-efficient methods for this process, which we will term as quantum-to-classical (Q2C) data decoding.

In this paper, we propose and evaluate a novel time-efficient Q2C approach based on sampling the output state using a multi-level decomposable Quantum Wavelet Transform (QWT) [6–8]. We also present optimized quantum circuits and accompanying circuit depth analysis for the proposed methods. Previously, multi-level decomposable QWT has been proven to be effective for reducing dimensionality of high-resolution spatio-spectral data [9] while maintaining spatial and temporal locality. When applied at the output of a quantum circuit, the resulting quantum state can be represented with fewer qubits by reducing it from a high-dimensional space to a lower dimensional space. Using empirical data, it will be shown that sampling the lower dimensional space can be performed in less time, thus improving the Q2C decoding process.

The proposed quantum method and circuits for Q2C are evaluated through simulation on the $ibmq_qasm_simulator$ [10] from IBM Quantum. By measuring circuit depth and execution time from experiments, a quantitative comparison of the proposed Q2C method with state-of-the-art techniques is presented. Additionally, the proposed Q2C method is compared with a reported Q2C readout technique based on the Quantum Fourier Transform (QFT) [11]. The experimental results show that our proposed methods are more time and space efficient, compared to existing methods.

The rest of the paper is organized as follows. Section II discusses some background concepts and related work. Section III presents the proposed method and quantum circuits. Section IV shows the experimental work and results. Finally, the conclusions of our work and a discussion of future work are included in Section V.

2 Background and Related Work

In this section, we will discuss the fundamental concepts of quantum gates and algorithms used in this paper and the related work on Q2C data decoding.

2.1 Quantum Gates

Hadamard Gate The Hadamard gate [11] is a single-qubit gate, described by (1), that forms superposition states when applied to qubits.

SWAP Gate A SWAP gate is a two-qubit quantum gate that swaps two qubits as described by (1).

$$H = \frac{1}{\sqrt{2}} \begin{bmatrix} 1 & 1 \\ 1 & -1 \end{bmatrix}; \quad SWAP = \begin{bmatrix} 1 & 0 & 0 & 0 \\ 0 & 0 & 1 & 0 \\ 0 & 1 & 0 & 0 \\ 0 & 0 & 0 & 1 \end{bmatrix}$$
 (1)

2.2 Quantum Wavelet Transform

Classical Discrete Wavelet Transform (DWT) uses non-sinusoidal functions called mother wavelets to decompose signals/data into their spatio-temporal spectral components [12] with high computational efficiency. The Haar is the simplest mother wavelet, which can be constructed using a unit step function, u(t) [8]. The equivalent algorithm of the Haar Transform in the quantum domain is the

Quantum Haar Transform (QHT) [6–8]. In QHT, input signal samples are encoded as the basis state coefficients of a quantum state $|\psi\rangle$ in superposition. The Haar function is applied on the coefficients, and the equivalent expression for the output of the QHT is given by (2), where Ψ_D is the discrete Haar mother wavelet [8], Δt is the sampling period, K is the Haar window size in samples, and N is the number of data samples. Corresponding quantum circuits for QHT can be constructed using Hadamard and SWAP gates [8].

$$|\psi\rangle_{\text{QHT}} = \frac{1}{\sqrt{N}} \sum_{j=0}^{N-1} \sum_{q=0}^{N-1} f(q \cdot \Delta t) \Psi_D\left(\frac{q-j}{K}\right) |j\rangle$$
 (2)

2.3 Related Work

A quantum-to-classical (Q2C) data decoding approach for image processing applications was proposed in [11]. The approach was based on extracting a collective property from the amplitudes of the quantum state by using Quantum Fourier Transform (QFT) and projecting the basis states in the frequency domain. Measurements in the Fourier bases provide us with information about the transformed image properties without decoding the actual output image pixels. This technique uses relatively fewer iterations/samples than used in the general approach. The data decoding method based on QFT is particularly interesting for image or audio processing applications, where the properties of the data such as spectral bandwidth are useful for analyzing the output [11]. The drawback of this technique is that it does not decode the actual data from its quantum state and reveals only the collective property or feature of data. Moreover, the timing overhead is also significantly large due to the complexity of the QFT circuit.

3 Proposed Methodology and Circuits

3.1 Methodology

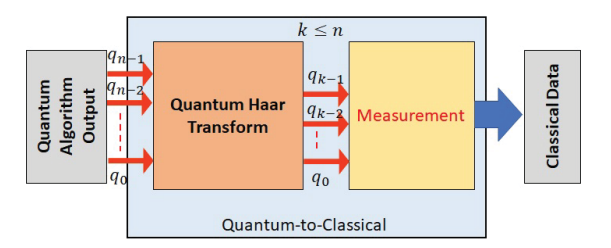


Fig. 1: Methodology overview for QHT-based quantum-to-classical data decoding.

One of the important features of the Quantum Haar Transform (QHT) is the preservation of the spatial and temporal locality of data [12]. Moreover, QHT is also decomposable for multiple levels. These features make QHT highly compatible for reducing data dimensionality while maintaining the spatial and/or temporal variation. Our proposed Q2C data decoding method employs the QHT

algorithm for dimension reduction. Using multi-level decomposable QHT, data represented by n qubits can be transformed to data with the similar spatial and temporal structures, but represented by a lower number of qubits k=(n-l.d), where l is the number of decomposition levels, and d is the dimensionality of the data. Thus, our goal of performing dimension reduction is to reduce the number of qubits for data representation and therefore to reduce the measurement and data decoding time. The proposed methodology for QHT-based Q2C data decoding is shown in Fig. 1.

3.2 Quantum Circuits

QHT is multi-level decomposable in either packet or pyramidal forms [8] and can be generalized for d-dimensional operations, denoted as $U^{d-D-QHT}$ hereafter.

d-dimensional QHT The operation $U^{d-D-QHT}$ is generalized for d-dimensional data using d Hadamard gates and permutations using SWAP gates [8]. Two variants of QHT, i.e., sequential and parallel QHT, were proposed in [8]. Our proposed Q2C method will use the most optimized and depth-efficient 1-stage parallel QHT circuit, denoted as $U_{par,opt}^{d-D-QHT}$, see Fig. 2a.

Packet Decomposition In packet decomposition of QHT, the operation $U^{d-D-QHT}$ is repeatedly applied for every level on qubits, and all qubits are required throughout the entire process. The circuit for packet decomposition is shown in Fig. 2b. The total circuit depth, given in (3), can be determined by the total number of SWAP operation levels and total number of Hadamard gate levels for each $U^{d-D-QHT}$ operation, times the number of decomposition levels.

$$\delta_{pkt} = ((n_{max} - 1) + 1) \cdot l = n_{max} \cdot l \tag{3}$$

where n_{max} is the maximum number of qubits in any dimension, and l is the number of decomposition levels.

Pyramidal Decomposition The circuit for pyramidal decomposition, denoted by $U_{pyramidal}^{d-D-QHT}$, is shown in Fig. 2c. In pyramidal decomposition, $U^{d-D-QHT}$ is applied on fewer data qubits for every level of decomposition. Specifically, d qubits (1 qubit per each dimension) are discarded after every decomposition level. The maximum number of possible pyramidal decomposition levels, l_{max}^{pyr} , is given by (4), where n is the total number of qubits, n_0 is the number of qubits representing data in the first dimension, and d is the dimensionality of the data.

$$l_{max}^{pyr} = \left\lfloor \min\left(\frac{n}{d}, 1 + \frac{n - n_0}{d - 1}\right) \right\rfloor \tag{4}$$

The advantage of using pyramidal over packet decomposition is that the size and depth of the QHT circuit are reduced after every decomposition level. However, one drawback is that additional inter-level permutations are required, see Fig. 2d. The total circuit depth, δ_{pyr} , for the multi-level pyramidal decomposition QHT circuit was calculated from Figs. 2b, 2c and 2d and is given in (5).

$$\delta_{pyr} = \delta_{pkt} + \delta_{pyr-perm} - \frac{l(l-1)}{2} \tag{5}$$

where $\delta_{pkt} = n_{max} \cdot l$ is the depth of packet decomposition, $\delta_{pyr-perm}$ is the total depth of overlapped inter-level permutations given by the expression in (6), and n_{max} is the maximum number of qubits in any dimension.

$$\delta_{pyr-perm} = \left(n - n_0 - (d-1)\left(\frac{l}{2}\right)\right)(l-1) \tag{6}$$

For pyramidal decomposition to be faster than packet decomposition, i.e. $\delta_{pyr} \leq \delta_{pkt}$, the term $\delta_{pyr-perm} - \frac{l(l-1)}{2}$ must be less than/equal to 0, see (5). Based on this condition, we determined the minimum number of decomposition levels, l_{min}^{pyr} shown in (7), for pyramidal to be faster than packet.

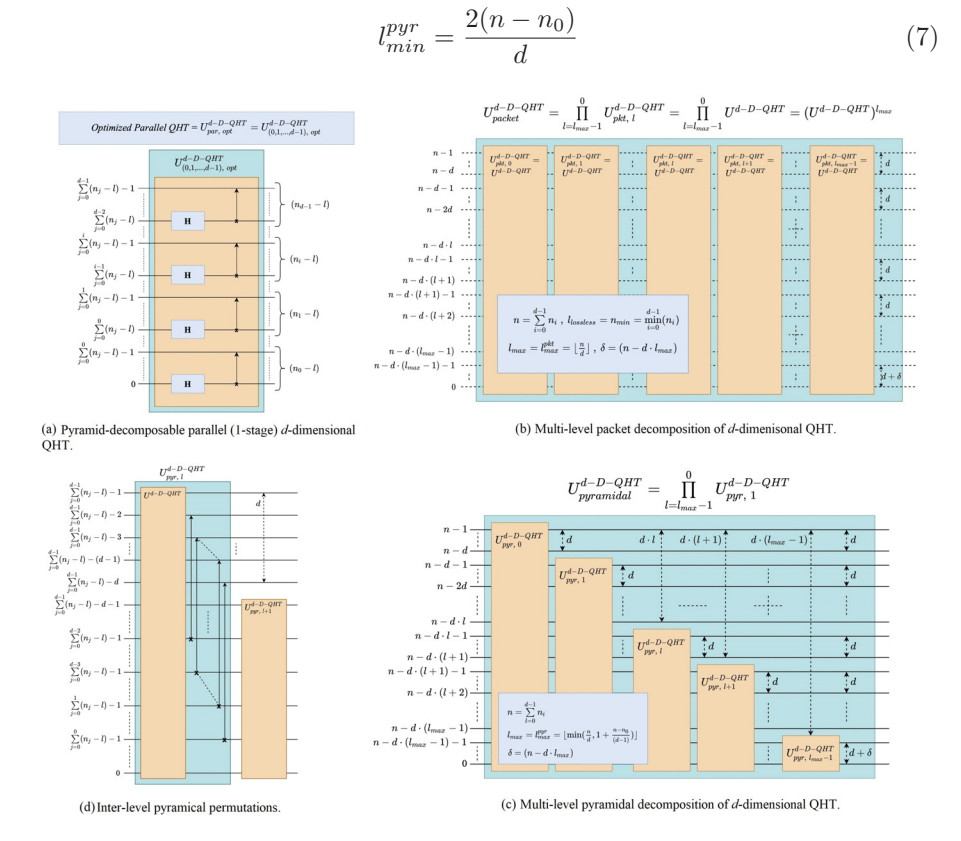


Fig. 2: Quantum circuits for multi-dimensional, multi-level decomposable Quantum Haar Transform [8].

4 Experimental Results

4.1 Setup

We conducted our experiments on IBM Quantum Lab [13] and used the built-in Qiskit [14] framework for implementing the proposed quantum circuits. Simulations of the developed circuits were performed using IBM's 32-qubit QASM simulator, *ibm_qasm_simulator* [13]. The number of circuit samples or shots for the experiments ranged from 1,024 to 16,384.

4.2 Quantum-to-Classical Experiments

Experimental evaluations of the proposed QHT-based Q2C method and the QFT-based approach reported in [11] were performed. The methods were evaluated in terms of overhead incurred and time efficiency.

Execution Time (ms)													
Number		Nu	mber of sh	ots									
of qubits	1024	2048	4096	8192	16384								
2	2.72	4.69	9.11	17.74	35.14								
4	3.35	6.64	12.86	27.32	51.76								
6	4.62	8.79	18.04	33.92	69.37								
8	6.11	10.86	20.71	40.83	84.29								
10	6.42	13.03	25.34	49.22	101.50								
12	7.61	14.75	29.55	58.37	117.58								
14	8.73	19.19	33.64	69.03	132.93								
16	9.78	19.05	38.17	77.40	155.60								
18	11.85	22.25	43.35	87.40	180.94								
20	12.42	24.16	49.62	96.05	191.52								
22	13.94	27.01	53.84	106.88	214.16								
24	15.06	29.65	61.77	119.33	239.15								
26	17.79	33.46	66.14	130.73	259.08								
28	19.05	35.30	71.14	141.06	281.05								
30	24.89	42.36	84.88	157.09	283.11								
32	28.40	46.53	90.30	167 50	327 12								

Table 1: Measurement timing data on IBM QASM simulator.

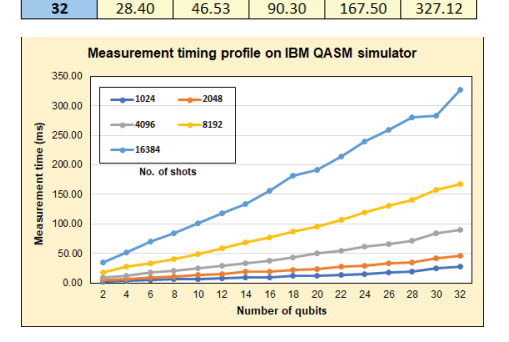


Fig. 3: Measurement time as a function of number of qubits and number of shots on IBM QASM Simulator.

Characterizing measurement (circuit sampling) time on IBM QASM We characterized the circuit sampling time on the IBM QASM simulator as a function of number of qubits and number of shots. Measurement gates were applied across ground state qubits and the number of qubits and shots were varied. The obtained execution times of the measurement gates (circuit sampling times) from the simulator are shown in Table 1 and Fig. 3. The measurement time increases linearly with the number of qubits for varying number of shots, as observed in Fig. 3. Based on the linear behavior, the measurement times for odd numbers of qubits in Table 1 were linearly interpolated from the graphs in Fig. 3 and used in the overhead analysis of the proposed Q2C method.

Simulation of Quantum Fourier Transform The QFT-based method for Q2C was evaluated by simulating n-qubit QFT circuits. The number of qubits, n, was varied from 2 to 28 and the number of shots was varied from 1,024 to 16,384, see Table 2. Larger circuit simulations could not be performed due to

simulator memory limitations. The obtained results were consistent with our theoretical expectations. The execution time increases exponentially with the number of qubits and this behavior is consistent for higher number of shots. The experimental data for QFT will be used for quantitative comparison with our proposed Q2C method.

Execution Time (ms)													
			Nu	mber of sh	ots								
Number of qubits	Circuit depth	1024	2048	4096	8192	16384							
2	5	6.75	9.51	17.42	24.56	39.15							
4	12	7.93	12.91	16.87	29.45	49.66							
6	23	11.15	15.27	25.79	32.85	64.02							
8	38	12.03	21.33	27.28	42.04	70.25							
10	57	15.95	19.64	25.97	47.02	93.53							
12	80	8.04	20.73	27.91	58.09	106.68							
14	107	20.71	35.04	41.41	61.37	126.11							
16	138	372.02	392.40	410.51	458.01	558.54							
18	173	446.00	521.30	533.46	479.67	577.21							
20	212	710.94	819.74	827.47	764.68	839.81							
22	255	1434.82	1495.12	1550.84	1482.87	1694.57							
24	302	4069.67	4234.29	4263.60	4218.60	4265.49							
26	353	15794.70	15683.52	15647.70	14368.76	14675.60							
28	408	49883.76	64556.78	65938.46	65019.31 70521.								
30 32	1	No data col	lected due	to simulato	r limitation	s							

Simulation of Quantum Haar Transform We evaluated our proposed QHT-based method of Q2C by simulating multi-level pyramidal decomposable 3D-QHT circuits varying the number of qubits, n from 4 to 32. For each n-qubit circuit, the number of pyramidal decomposition levels was varied from 1 to l_{max} , see (4), and we obtained circuit depth measurements and circuit execution times. All data was collected for 16,384 shot simulations. The multi-level QHT circuits were highly optimized, resulting in significantly lower circuit depths compared to QFT which is consistent with our theoretical expectations, see Table 3. Moreover, the simplistic nature of quantum gates in the QHT circuit such as SWAP gates, as compared to controlled phase shift gates in the QFT [15], should theoretically incur lower execution time. Table 4 presents the execution timing data obtained

Table 3: Multi-level 3D Quantum Haar Transform circuit depths compared to QFT circuit depths.

	Circuit depth														
Number of qubits	QFT					3D-	QHT								
2 4 6 8 10 12 14	·	1-level	2-level	3-level	4-level	5-level	6-level	7-level	8-level	9-level	10-level				
2	5														
4	12	3													
6	23	7	12												
8	38	11	20												
10	57	15	28	37											
12	80	19	36	49	59										
14	107	22	42	58	71										
16	138	24	46	64	79	91									
18	173	26	50	70	87	101	112								
20	212	28	54	76	95	111	124								
22	255	30	58	82	103	121	136	148							
24	302	31	59	85	107	126	142	155	165						
26	353	31	59	84	106	126	142	155	165						
28	408	31	59	84	106	125	141	155	165	172					
30	No data collected due to simulator	31	59	84	106	125	141	154	164	172	176				
32	limitations	31	59	84	106	125	141	154	164	171	175				

from multi-level 3D-QHT simulations on IBM Quantum. For comparison, also

011	11011	- «	11		1 01	m.	Lauc	,,	•																			
shots = 16,384		QFT													3D-QH	т												
Number	n-qubit		\vdash		1-lev	rel		т		2-leve	el		т		3-leve			т		4-leve			5-level					
of qubits,	t _{measure} (ms)	t _{exec} (ms)	k	t _{exec} (ms)	k-qubit t _{ressure} (ms)	t _{total} (ms)	Speedup	k	t _{exec} (ms)	k-qubit t _{measure} (ms)	t _{total} (ms)	Speedup	k	t _{exec} (ms)	k-qubit t _{measure} (ms)	t _{total} (ms)	Speedup	k	t _{exec} (ms)	k-qubit t _{rressure} (ms)	t _{total} (ms)	Speedup	k	t _{exec} (ms)	k-qubit t _{measure} (ms)	t _{total} (ms)	Speedup	
2	35.14	39.15																										
4	51.76	49.66	1	0.34	17.57	17.91	2.89																					
6	69.37	64.02	3	0.29	43.45	43.74	1.59																					
8	84.29	70.25	5	0.28	60.57	60.85	1.39	2	0.41	35.14	35.55	2.37																
10	101.50	93,53	7	0.30	76.83	77.13	1.32	4	0.46	51.76	52.22	1.94	1	0.63	17.57	18.20	5.58	Т					Г					
12	117.58	106.68	9	0.32	92.90	93.22	1.26	6	0.47	69.37	69.84	1.68	3	0.74	43.45	44.19	2.66											
																							Н					
14	132.93	126.11	11	0.33	109.54	109.87	1.21	8	0.57	84.29	84.86	1.57	5	0.58	60.57	61.14	2.17	2	0.65	35.14	35.79	3.71						
16	155.60	558.54	13	0.43	125.26	125.68	1.24	10		101.50	102.23		7	0.78	76.83	77.61	2.00	4	0.68	51.76	52.44	2.97	1	0.86	17.57	18.43	8.44	
18	180.94	577.21	15	0.49	144.27	144.75	1.25	12	0.68	117.58	118.26	1.53	9	0.84	92.90	93.73	1.93	6	0.73	69.37	70.10	2.58	3	0.92	43.45	44.37	4.08	
20	191.52	839.81	17	0.48	168.27	168.75	1.13	14	0.83	132.93	133.76	1.43	11	0.91	109.54	110.45	1.73	8	0.81	84.29	85.10	2.25	5	1.09	60.57	61.65	3.11	
22	214.16	1694.57	19	0.59	186.23	186.82	1.15	16	0.93	155.60	156.53	1.37	13	0.91	125.26	126.17	1.70	10	0.92	101.50	102.42	2.09	7	1.19	76.83	78.02	2.74	
24	239.15	4265.49	21	0.83	202.84	203.67	1.17	18	0.97	180.94	181.91	1.31	15	1.10	144.27	145.36	1.65	12	0.95	117.58	118.53	2.02	9	1.19	92.90	94.09	2.54	
26	259.08	14675.60	23	0.79	226.66	227.44	1.14	20	0.86	191.52	192.38	1.35	17	1.12	168.27	169.39	1.53	14	1.26	132.93	134.19	1.93	11	1.29	109.54	110.83	2.34	
28	281.05	70521.61	25	0.74	249.12	249.85	1.12	22	0.89	214.16	215.05	1.31	19	1.13	186.23	187.36	1.50	16	1.07	155.60	156.67	1.79	13	1.30	125.26	126.56	2.22	
30	283.11	No data collected due	27	0.89	270.07	270.95	1.04	24	0.96	239.15	240.11	1.18	21	1.05	202.84	203.89	1.39	18	1.03	180.94	181.97	1.56	15	1.44	144.27	145.70	1.94	
32	327.12	to simulator limitations	29	0.94	282.08	283.02	1.16	26	1.18	259.08	260.26	1.26	23	1.04	226.66	227.70	1.44	20	1.48	191.52	193.00	1.69	17	1.45	168.27	169.72	1.93	
shots = 16,384		QFT													3D-QH	т												
Number	n-qubit				6-lev	rel				7-leve	el				8-leve	el				9-leve	d				10-lev	el		
of	t _{measure} (ms)	t _{exec} (ms)			k-qubit					k-qubit					k-qubit					k-qubit					k-qubit			
qubits,	(5)	Sexec (IIIs)	k	t _{exec} (ms)	t _{measure}	t _{total} (ms)	Speedup	k	(ms)	t _{measure}	t _{total} (ms)	Speedup	k	t _{exec} (ms)	t _{measure}	t _{total} (ms)	Speedup	k	(ms)	tmeasure	t _{total} (ms)	Speedup	k	(ms)	tmeasure	t _{total} (ms)	Speedup	
n				,	(ms)				,	(ms)	,,			,	(ms)	,,,,,,,				(ms)				,,	(ms)	,		
20	191.52	839.81	2	1.10	35.14	36.24	5.28																					
22	214.16	1694.57	4	1.27	51.76	53.03	4.04	1	1.38	17.57	18.95	11.30																
24	239.15	4265.49	6	1.42	69.37	70.79	3.38	3	1.35	43.45	44.80	5.34																
26	259.08	14675.60	8	1.50	84.29	85.79	3.02	5	1.35	60.57	61.92	4.18	2	2.09	35.14	37.23	6.96											
28	281.05	70521.61	10	1.41	101.50	102.91	2.73	7	1.71	76.83	78.54	3.58	4	2.01	51.76	53.77	5.23	1	1.67	17.57	19.24	14.61						
30	283 11	No deta	12	1 34	117 58	118 97	2.38		153	92.90	94.43	3.00	6	1.67	69 37	71.04	3 99	3	1.70	43.45	45.15	6.27						

Table 4: Multi-level 3D-QHT execution times compared to QFT simulation times on IBM QASM simulator.

presented in Table 4 are the *n*-qubit measurement timing data, which is the execution time of only measurement gates (without QFT or QHT) obtained from Table 1, and *n*-qubit QFT circuit execution timing data from Table 2.

For every l^{th} -level 3D-QHT decomposition, $l=1,2,...,l_{max}$, the QHT circuit execution times, the reduced number of qubits k, and the corresponding k-qubit measurement times are also shown in Table 4. From this data we calculate the total time for l^{th} -level QHT as the sum of the QHT circuit execution time and the corresponding k-qubit measurement time. In Table 4 we also present the speedup of QHT-based total time relative to general n-qubit measurement time (without QFT or QHT), see (8).

Speedup =
$$\frac{t_{measure}(n)}{t_{measure}(k) + t_{exec}^{QHT}(n, l)} = \frac{t_{measure}(n)}{t_{total}^{QHT}(n, l)}$$
(8)

where $t_{measure}(n)$ and $t_{measure}(k)$ are the measurement times without QFT or QHT for n-qubits and k-qubits, respectively, $t_{exec}^{QHT}(n,l)$ is the execution time for n-qubit l-level QHT, and $t_{total}^{QHT}(n,l)$ is the total time.

4.3 Analysis of Results

The QFT or the multi-level QHT-based methods incur overhead in the overall measurement time due to the additional QFT or QHT circuits, respectively. Using the data obtained from our experiments, we characterized the timing overheads of both methods. We also determined the speedup gained by use of the

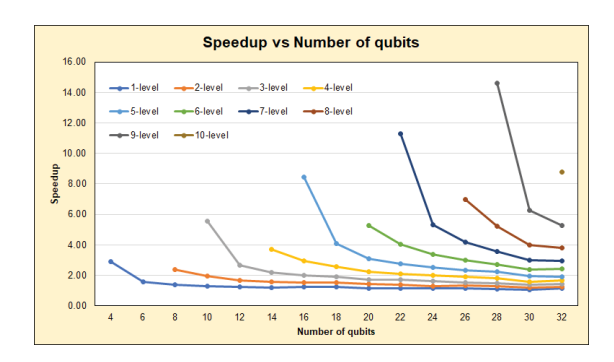


Fig. 4: Speedup of the proposed multi-level QHT based Q2C method as a function of number of qubits.

proposed QHT-based method relative to the general measurement method without QFT or QHT. For example, considering the data in Table 4, the measurement time for a 28-qubit circuit sampled for 16,384 shots is 281.05ms. If QFT-based sampling is applied, the equivalent 28-qubit QFT circuit adds a large overhead of 70s. Assuming that the number of shots required is now 1024 as a result of QFT sampling, the reduction in measurement time from 16,384 shots to 1,024 shots, see Table 1, is much less compared to the increased overhead due to the added 28-qubit QFT circuit, see Table 2. Therefore, the overall effect is an increase in total execution time. Using our proposed multi-level QHT-based sampling for the case when n=28 and l=4, the number of qubits is reduced from n=28 to k=16, see Table 4. The reduced time taken for measurement is now 155.60ms, while the additional overhead of 4-level 3D-QHT is 1.07ms. Therefore the total time is 156.67ms, which is a 44.4% reduction relative to the time taken (281.05ms) for measuring all 28 qubits, and equivalent to a speedup of $\times 1.79$. For n = 32, the maximum number of decomposition levels l_{max}^{pyr} , is 10, and applying 10-level 3D-QHT results in a ×8.80 speedup in measurement time. The speedup gained by our proposed QHT-based Q2C method relative to the general measurement is presented as a function of number of qubits in Fig. 4 for different levels of 3D-QHT decomposition. It is worth mentioning that for a fixed level of decomposition, the speedup decreases with increase in the number of qubits, see Fig. 4. This is because for large number of qubits n, the measurement times of k qubits become very close to the n-qubit measurement times, and the overhead due to QHT becomes relatively negligible such that the speedup asymptotically approaches unity, see (8). However, for a fixed number of qubits the speedup increases, as expected, with increase in the number of decomposition levels, see Fig. 4.

5 Conclusions and Future Work

Existing quantum-to-classical (Q2C) data decoding methods incur significant overhead in circuit execution times and makes the practical implementation of time-efficient quantum algorithms challenging. In this work, we proposed time-

efficient methods for Q2C data decoding. Depth-optimized, multi-level decomposable Quantum Haar Transform (QHT) circuits were also proposed for Q2C data decoding. The quantum circuits were evaluated experimentally on the IBM Quantum platform. Implementation of related methods were also performed for quantitative analysis. The experimental evaluations showed that the proposed methods were consistent with theoretical expectations and improved the time efficiency of the Q2C processes. Future work will include investigating further optimizations for the proposed Q2C methods, and integrating quantum error correction methods for improving fidelity.

References

- Rønnow, T.F., Wang, Z., Job, J., Boixo, S., Isakov, S.V., Wecker, D., Martinis, J.M., Lidar, D.A., Troyer, M.: Defining and detecting quantum speedup. science 345(6195), 420–424 (2014)
- Guan, W., Perdue, G., Pesah, A., Schuld, M., Terashi, K., Vallecorsa, S., Vlimant, J.R.: Quantum machine learning in high energy physics. Machine Learning: Science and Technology 2(1), 011,003 (2021)
- 3. Preskill, J.: Quantum computing in the nisq era and beyond. Quantum 2, 79 (2018)
- 4. Weigold, M., Barzen, J., Leymann, F., Salm, M.: Data encoding patterns for quantum computing. In: HILLSIDE Proc. of Conf. on Pattern Lang. of Prog. 22 (2020)
- Lanzagorta, M., Uhlmann, J.: Is quantum parallelism real? In: Quantum Information and Computation VI, vol. 6976, p. 69760W. International Society for Optics and Photonics (2008)
- 6. Fijany, A., Williams, C.P.: Quantum wavelet transforms: Fast algorithms and complete circuits. In: NASA international conference on quantum computing and quantum communications, pp. 10–33. Springer (1998)
- 7. Li, H.S., Fan, P., Peng, H., Song, S., Long, G.L.: Multilevel 2-d quantum wavelet transforms. IEEE Transactions on Cybernetics (2021)
- 8. Mahmud, N., Macgillivray, A., Chaudhary, M., El-Araby, E.: Decoherence-optimized circuits for multi-dimensional and multi-level decomposable quantum wavelet transform. IEEE Internet Computing (IEEE IC) Special Issue on Quantum and Post-Moore's Law Computing 26(01), 15–25 (2022)
- 9. Mahmud, N., Haase-Divine, B., MacGillivray, A., El-Araby, E.: Quantum dimension reduction for pattern recognition in high-resolution spatio-spectral data. IEEE Transactions on Computers **71**(1), 1–12 (2020)
- 10. IBM: QasmSimulator Qiskit 0.36.1 documentation. https://qiskit.org/documentation/stubs/qiskit.providers.aer.QasmSimulator.html (2022). [Online] Accessed: 2022-06-13
- 11. Williams, C.P., Clearwater, S.H.: Explorations in quantum computing. Springer (1998)
- 12. El-Araby, E., El-Ghazawi, T., Le Moigne, J., Gaj, K.: Wavelet spectral dimension reduction of hyperspectral imagery on a reconfigurable computer. In: Proceedings. 2004 IEEE International Conference on Field-Programmable Technology (IEEE Cat. No. 04EX921), pp. 399–402. IEEE (2004)
- 13. IBM: IBM Quantum Services. https://quantum-computing.ibm.com/services (2022). [Online] Accessed: 2022-06-13
- 14. Wille, R., Van Meter, R., Naveh, Y.: Ibm's qiskit tool chain: Working with and developing for real quantum computers. In: 2019 Design, Automation & Test in Europe Conference & Exhibition (DATE), pp. 1234–1240. IEEE (2019)
- 15. Nielsen, M.A., Chuang, I.: Quantum computation and quantum information (2002)